Supporting Information

Determination of organic arsenic acids by machine learning assisted SERS on silicon modifiedlicon modified coating of Fe_3O_4@Ag

Ziqi Zhang† [1,2], Jianrong Tian† [1,2], Huaqing Ling[1,2], Zhixi Zhao[1,2,3], Shan Chen[1,2], Zulihaya Maimaiti[1,2], Yufang Ye[1], Qing Wang[1], Yongbin Li[4]

[1]College of Chemistry and Chemical Engineering, Xinjiang Normal University, Urumqi 830000, China

[2]Xinjiang Key Laboratory of Energy Storage and Photoelectroctalytic Materials, Urumqi 830000, China

[3]Technical Research Center for Environmental Geotechnical Engineering Restoration and Resource Utilization, Xinjiang Normal University, Urumqi 830054, China

[4]School of Environment Science, Dalian University of Technology, Dalian 116000, China

The stability of the substrate was calculated from the relative standard deviation (RSD).

According to the relative standard deviation (RSD):

$$RSD = S \div \overline{X} \times 100\% \qquad \text{(S1)}$$

where S was calculated as follows: $S = \sqrt{\frac{\sum_{i=1}^{n}\left(x_i - \overline{x}\right)^2}{n-1}}$

where S was the standard deviation of the spectral intensity and $\overline{X}$ was the corresponding mean value.

The Analytical Enhancement Factor (AEF) stood as a pivotal metric in assessing the SERS efficacy of a substrate[1]. AEF was calculated using Equation S2, which represents

$$EF = \frac{I_{SERS}}{N_{SERS}} \times \frac{N_{\mathrm{NR}}}{I_{\mathrm{NR}}} \qquad \text{(S2)}$$

Where, I_{SERS} represents the signal intensity of the characteristic peak of organic arsenic acid (500.0 μg/L) measured utilizing $Fe_3O_4@SiO_2@Ag$ NPs as the SERS substrate, and N_{SERS} denotes the count of effective organic arsenic acid molecules on the surface of the $Fe_3O_4@SiO_2@Ag$ NPs substrate under irradiation. I_{NR} is the Raman signal intensity of the organic arsenic acid at a concentration of 1 mol/L, and N_{NR} dis the count of effective organic arsenic acid molecules illuminated by the laser spot.

$$\mathrm{Accuracy} = 100 \times \frac{\mathrm{Ture\ Positives} + \mathrm{Ture\ Negatives}}{\mathrm{Ture\ Positives} + \mathrm{Ture\ Negatives} + \mathrm{False\ Positives} + \mathrm{False\ Negatives}} \qquad \text{(S3)}$$

$$\mathrm{Sensitivity} = 100 \times \frac{\mathrm{Ture\ Positives}}{\mathrm{Ture\ Positives} + \mathrm{False\ Negatives}} \qquad \text{(S4)}$$

$$\mathrm{Specificity} = 100 \times \frac{\mathrm{Ture\ Negatives}}{\mathrm{Ture\ Negatives} + \mathrm{False\ Positives}} \qquad \text{(S5)}$$

$$\mathrm{Precision} = 100 \times \frac{\mathrm{Ture\ Positives}}{\mathrm{Ture\ Positives} + \mathrm{False\ Positives}} \qquad \text{(S6)}$$

Table S1 Mass yield of each synthesis step for Fe_3O_4@SiO_2@Ag nanoparticles

Synthesis Step	Starting Material	Starting Mass (g)	Theoretical Mass (g)	Product Mass (g)	Yield (%)
Step 1: Fe_3O_4	$FeCl_3·6H_2O$	2.1	0.60	0.47	78.3%
Step 2: SiO_2 coating	Fe_3O_4	0.2	0.37	0.23	62.2%
Step 3: Ag	Fe_3O_4@SiO_2	0.05	0.17	0.15	88.2%

*Theoretical basis is calculated based on stoichiometric ratios

Table S2 Peak coordination of DMA and ROX in normal Raman and SERS spectra

Assignments	Cacodylic acid$(cm)^{-1}$		Roxarsone$(cm)^{-1}$		Ref
	Normal Raman	SERS	Normal Raman	SERS	
v(As-C)	/	/	619	622	2
v_s(As-OH)	/	/	750	/	
v(AsOx)	/	/	809	799	
$v_s(NO_2)$	/	/	1335	1323	
v(As-C)	598,633	610, 640	637	633	3
v_s(As-OH)	777	749	744	700	
v_s, v_{as}(As=O)	816	832	862	824	
$V_s(NO_2)$	/	/	1263	1332, 1356	
v(As-C)	/	/	637	627	4
v_s(As-OH)	/	/	744	/	
v(AsOx)	/	/	824	797	
$v_s(NO_2)$	/	/	1342	1322	
v(As-C)	658	/	/	/	5
v_s(As-OH)	752	/	/	/	
v(As-C)	/	600	/	/	6
v(As-O)	/	830	/	/	
v(As-C)	634	666	619	617	This work
v_s(As-OH)	755	803	/	/	
v(AsOx)	/	/	810	797	
$v_s(NO_2)$	/	/	1332	1334	

Table S3 Composition of natural surface water samples

Composition	ρ(mg/L)	Composition	ρ(mg/L)
K^+	2.918	Cl^-	12.309
Na^+	52.014	SO_4^{2-}	214.320
Ca^+	87.829	HCO_3^-	196.114
Mg^+	27.966	NO_3^-	2.210

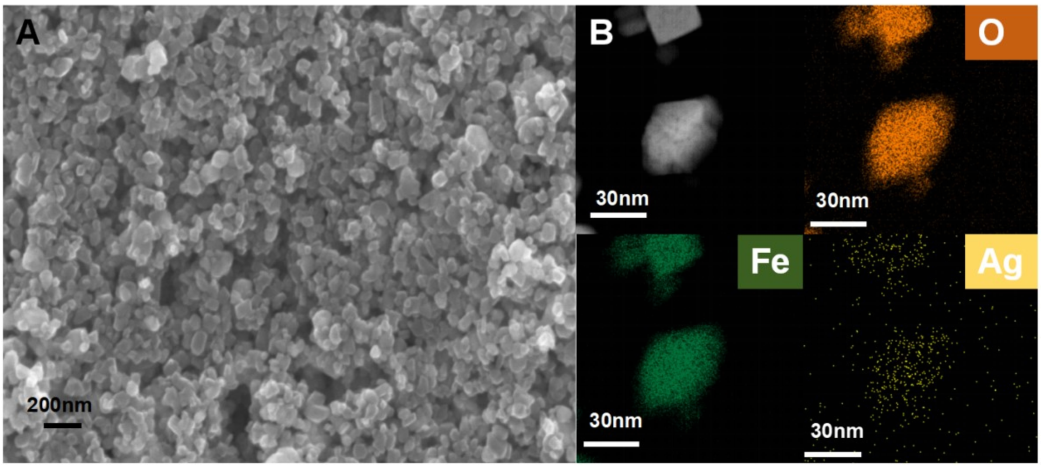

Fig. S1 Characterization of Fe_3O_4@Ag. SEM image(A), TEM image of Fe_3O_4@Ag (B) elemental analysis of energy dispersive spectroscopy (EDS)

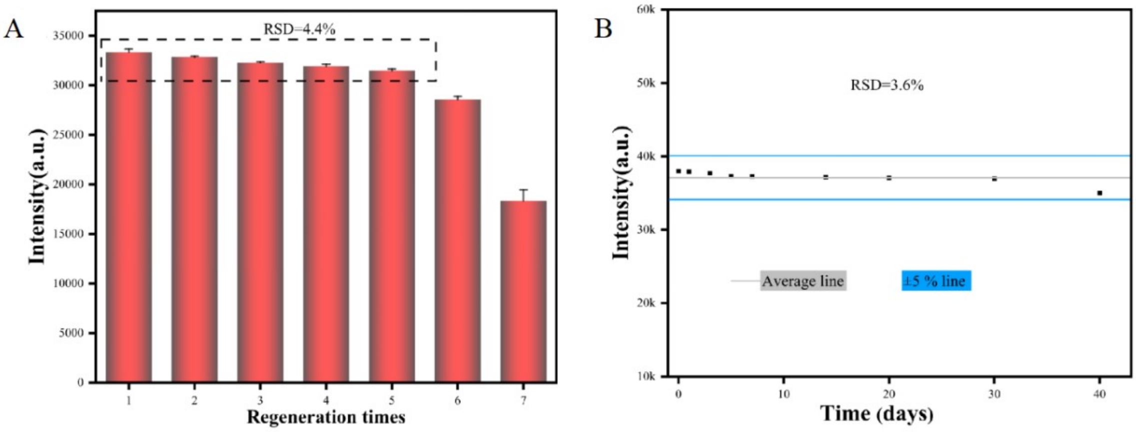

Fig. S2 Regeneration test of $Fe_3O_4@SiO_2$@Ag (A) and stability of the $Fe_3O_4@SiO_2$@Ag (B).

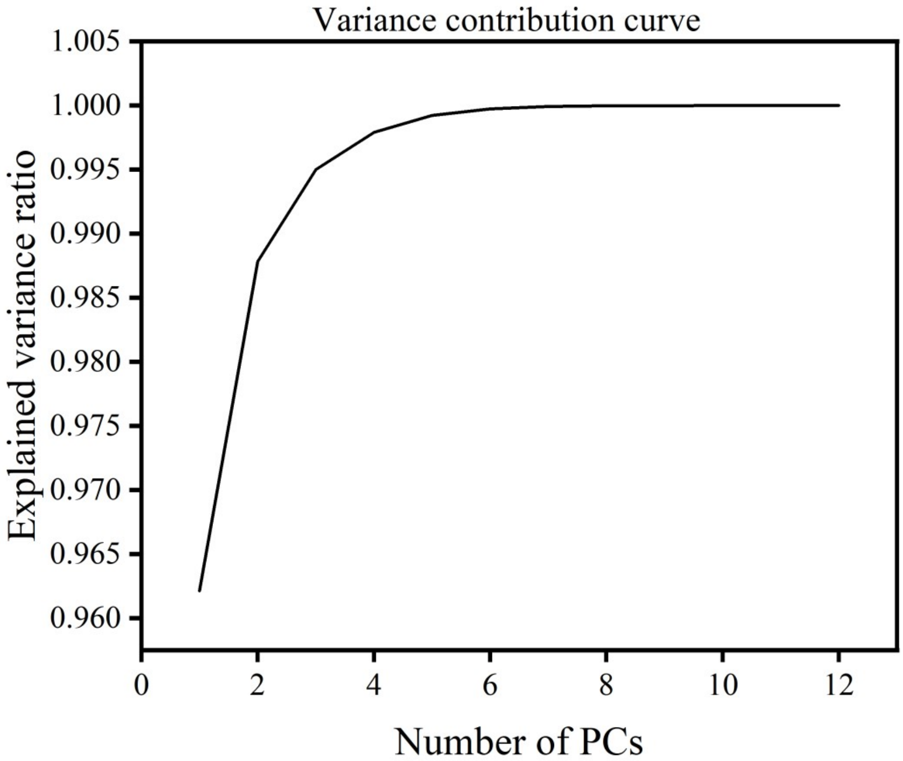

Fig. S3 The contribution rate of the principal component characteristic variance

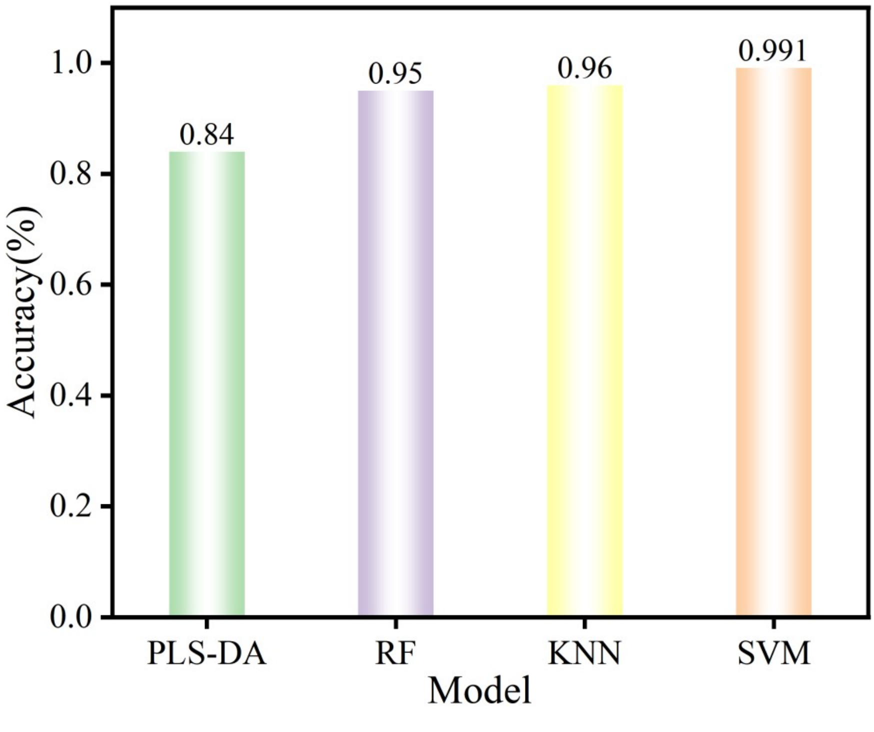

Fig. S4 Classification accuracies of four machine learning models

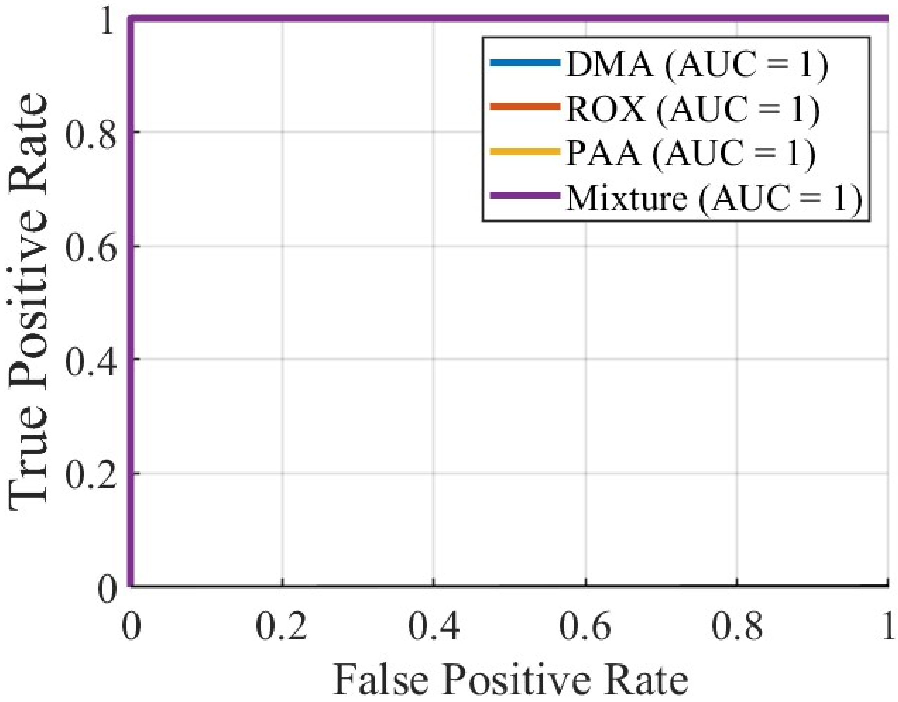

Fig. S5 ROC curve of validation set result by the trained support vector machinest model

Reference

1. E. Cara, L. Mandrile, A. Sacco, A. M. Giovannozzi, A. M. Rossi, F. Celegato, N. De Leo, P. Hönicke, Y. Kayser, B. Beckhoff, D. Marchi, A. Zoccante, M. Cossi, M. Laus, L. Boarino and F. Ferrarese Lupi, J MATER CHEM C, 2020, 8, 16513-16519. http://doi.org/10.1039/D0TC04364H.
2. J. Olavarría-Fullerton, S. Wells, W. Ortiz-Rivera, M. J. Sepaniak and M. A. De Jesus, APPL SPECTROSC, 2011, 65, 423-428. https://10.1366/10-06116.
3. R. López, F. J. Pereira, D. Suarez and A. J. Aller, MICROCHEM J, 2022, 175, 107186. https://doi.org/10.1016/j.microc.2022.107186.
4. S. Xu, F. P. Sabino, A. Janotti, D. B. Chase, D. L. Sparks and J. F. Rabolt, The Journal of Physical Chemistry A, 2018, 122, 9474-9482. https://doi.org/10.1021/acs.jpca.8b09104
5. S. Cowen, M. Duggal, T. Hoang and H. A. Al-Abadleh, CAN J CHEM, 2008, 86, 942-950. https://doi.org/10.1139/v08-102
6. M. Yang, V. Liamtsau, C. Fan, K. L. Sylvers, A. J. McGoron, G. Liu, F. Fu and Y. Cai, ANAL CHEM, 2019, 91, 8280-8288. https://10.1021/acs.analchem.9b00999.